

Predictive Capabilities of Cubic Turbulence Model in the Square Duct

Honoré Gnanga^{a,b}, Zita H. Moussambi Membetsi^b,
Roger Ondo Ndong^b, Hugues M. Omanda^b, Zaynab Salloum^{a,c}

^a*Université des Sciences et Technologies de Lille,
Polytech-Lille LML – UMR CNRS 8107, Boulevard P. Langevin,
59655 Villeneuve d'Ascq, France*

^b*Ecole Normale Supérieure de Libreville,
GABON Laboratoire Pluridisciplinaire de Sciences (LAPLUS)*

^c*Université Libanaise, Faculté des Sciences,
Département des Mathématiques, Beyrouth, Liban*

Abstract

The aim of this work is to predict numerically the turbulent flow through a straight square duct. The numerical simulations using Reynolds Averaged Navier-Stokes equations with a cubic eddy-viscosity turbulence model. This model has been devised by Craft, Launder and Suga (1996). The paper deals with a priori evaluation and improvement of the Explicit Algebraic Reynolds Stress model (EARSM) in order to assess its predictive capabilities in the simulation of a fully turbulent flow through a straight square duct. In order to handle wall proximity effects, damping functions are introduced. The comparison of the numerical results with available DNS shows good agreements.

Key words: turbulence modeling, cubic model, realizability, dumping functions

Introduction

The turbulence flow inside a duct of square cross-section is of considerable engineering interest. This flow is characterized by the existence of secondary flows which can be classified into two types, namely, Prandtl's flows of the first and second Kind. In general, numerical predictions of turbulent flows have become a valuable tool to obtain a detailed description of the turbulent flows which are difficult to obtain experimentally. Attempts to predict the turbulent characteristics have resulted in

several computational approaches. This work focuses on a numerical investigation of a low Reynolds number turbulent flow through a square duct with emphasis on Explicit Algebraic Reynolds Stress model (EARSM) which are based on the general constitutive equations and which has been derived by Craft et al. (1996) [1]. This EARSM model has been proposed to extend the applicability of many quadratic models [2]. Note that, this model [1] is a cubic relation between the strain and vorticity tensor and the stress tensor, and according these authors, it seems most appropriate to reflect the effects of curvature and swirling. Therefore, the present study aims at investigating the capability of this cubic viscosity turbulence model in the fully turbulence flow through a straight square duct. This square duct configuration has been frequently chosen by many authors [3, 4, 5] since it is a relatively simple geometry which provides a good case test to improve turbulence models.

The paper is organised as follows: The EARSM model herein employed is briefly supplied in section 2. The main results of this work are presented and discussed in section 3. This is followed by conclusions drawn from the present predictions.

Governing equations

In the present work, RANS formulation is used to predict the turbulent flow. This approach is used applying the Reynolds decomposition, which consists in splitting velocity and pressure into an average and a fluctuating part. The equations governing the mean velocity \bar{U}_i and mean pressure \bar{P} are obtained from the RANS equations for incompressible flow:

$$\frac{\partial \bar{U}_i}{\partial x_i} = 0 \quad (1)$$

$$\frac{\partial \bar{U}_i}{\partial t} + \frac{\partial}{\partial x_j} (\bar{U}_i \bar{U}_j) - \frac{\partial}{\partial x_j} \left(\nu \frac{\partial \bar{U}_i}{\partial x_j} - \overline{u_i u_j} \right) + \frac{1}{\rho} \frac{\partial \bar{P}}{\partial x_i} = 0 \quad (2)$$

where ρ is the fluid density, ν is the cinematic viscosity and $\overline{u_i u_j}$ is the Reynolds stress tensor. The indices $i, j, k = 1, 2, 3$ refer to the x, y, and z directions, respectively; x is the streamwise and y and z are the transverse directions.

To close the RANS equations (1) and (2), the cubic eddy-viscosity model of turbulence proposed by Craft et al. (1996) [1] is used. The most general such expression retaining terms up to cubic level that satisfies the required symmetry and contraction properties, can be written as follows:

$$\begin{aligned}
 \overline{u_i u_j} = & \frac{2}{3} k \delta_{ij} - \nu_t S_{ij} + c_1 \frac{\nu_t k}{\varepsilon} (S_{ik} S_{jk} - 1/3 S_{kl} S_{ij}) \\
 & + c_2 \frac{\nu_t k}{\varepsilon} (\Omega_{ik} S_{jk} + \Omega_{jk} S_{ik}) + c_3 \frac{\nu_t k}{\varepsilon} (\Omega_{ik} \Omega_{jk} - 1/3 \Omega_{kl} \Omega_{ij}) \\
 & \longleftarrow \text{quadratic terms} \longrightarrow \\
 & + c_4 \frac{\nu_t k^2}{\varepsilon} (S_{ki} \Omega_{ij} + S_{ij} \Omega_{ki}) S_{kj} + c_5 \frac{\nu_t k^2}{\varepsilon} (\Omega_{il} \Omega_{lm} S_{mj} + S_{il} \Omega_{lm} \Omega_{nj} - 2/3 S_{lm} \Omega_{mn} \Omega_{nl} \delta_{ij}) \\
 & + c_6 \frac{\nu_t k^2}{\varepsilon} S_{ij} S_{kl} S_{kl} + c_7 \frac{\nu_t k^2}{\varepsilon} S_{ij} \Omega_{kl} \Omega_{kl} \\
 & \longleftarrow \text{cubic terms} \longrightarrow
 \end{aligned} \tag{3}$$

where k ($= \overline{u_i u_i} / 2$) is the turbulent kinetic energy, ν_t ($= C_\mu f_\mu k^2 / \varepsilon$) is the turbulent viscosity, $\tilde{\varepsilon}$ ($= \varepsilon - 2\nu(\partial k^{1/2} / \partial x_j)^2$) is the ‘‘isotropic’’ dissipation rate, δ_{ij} is the Kronecker tensor, and S_{ij} and Ω_{ij} are the mean rate of deformation and vorticity tensors. These they are defined by:

$$\begin{aligned}
 S_{ij} &= (\partial \overline{U}_i / \partial x_j + \partial \overline{U}_j / \partial x_i) / 2 \\
 \Omega_{ij} &= (\partial \overline{U}_i / \partial x_j - \partial \overline{U}_j / \partial x_i) / 2
 \end{aligned} \tag{4}$$

with

$$f_\mu = 1 - \exp[-(\text{Re}_t / 90)^{1/2} - (\text{Re}_t / 400)^2] \tag{5}$$

Re_t ($= k^2 / \nu \tilde{\varepsilon}$) is the turbulent Reynolds number, ε is the dissipation rate of the turbulent kinetic energy. The model coefficients C_1 , C_2 , C_3 , C_4 , C_5 , C_6 and C_7 of equation (3), proposed by Craft et al. (1996) [1], are given in the Table 1.

Table 1: The proposed form for the coefficients of equation 3

C_1	C_2	C_3	C_4	C_5	C_6	C_7
-0.1	0.1	0.26	$-10c_\mu^2$	0	$-5c_\mu^2$	$5c_\mu^2$

where the coefficient C_μ is a function of the strain and vorticity invariants \tilde{S} and $\tilde{\Omega}$:

$$C_\mu = \frac{0.3}{1 + 0.35 \left(\max(\tilde{S}, \tilde{\Omega}) \right)^{3/2}} \left(1 - e^{\left[\frac{-0.36}{-0.75 \left(\max(\tilde{S}, \tilde{\Omega}) \right)} \right]} \right) \tag{6}$$

The nondimensional strain rate \tilde{S} and vorticity $\tilde{\Omega}$ are denoted by:

$$\tilde{S} = k / \tilde{\varepsilon} \sqrt{S_{ij} S_{ij} / 2}, \quad \tilde{\Omega} = k / \tilde{\varepsilon} \sqrt{\Omega_{ij} \Omega_{ij} / 2} \tag{7}$$

The cubic stress-strain relation (3) adopted here presents some advantages. Indeed, the quadratic terms and strain/vorticity-dependent coefficients are responsible

for the ability of non-linear models to capture anisotropy, and the cubic terms can reflect the effect of curvature. Also, these cubic terms can capture the swirling effect [6].

The turbulence energy k and the “isotropic” dissipation rate $\tilde{\varepsilon}$ are obtained from the following transport equations:

$$\frac{Dk}{Dt} = P_k - \varepsilon + \frac{\partial}{\partial x_j} \left[\left(\nu + \frac{\nu_t}{\sigma_k} \right) \frac{\partial k}{\partial x_j} \right] \quad (8)$$

$$\frac{D\tilde{\varepsilon}}{Dt} = c_{\varepsilon 1} \frac{\tilde{\varepsilon}}{k} P_k - c_{\varepsilon 2} \frac{\tilde{\varepsilon}^2}{k} + E + Y_{ap} + \frac{\partial}{\partial x_j} \left[\left(\nu + \frac{\nu_t}{\sigma_\varepsilon} \right) \frac{\partial \tilde{\varepsilon}}{\partial x_j} \right] \quad (9)$$

where $\frac{D(\cdot)}{Dt} = \frac{\partial(\cdot)}{\partial t} + \overline{U_j} \frac{\partial(\cdot)}{\partial x_j}$ is the material derivative, $P_k = -\overline{u_i u_j} \frac{\partial \overline{U_i}}{\partial x_j}$ is the turbulent production.

The near-wall extra term E employed by Suga [7] can be written as:

$$\begin{cases} E = 0.0022 \frac{\tilde{S} \nu_t k^2}{\varepsilon} \left(\frac{\partial^2 \overline{U_i}}{\partial x_j \partial x_k} \right) & \text{if } Re_i \leq 250 \\ E = 0 & \text{if } Re_i > 250 \end{cases} \quad (10)$$

The length-scale correction Y_{ap} proposed by Yap [8] can be expressed as follows:

$$Y_{ap} = 0.83 \frac{\tilde{\varepsilon}^2}{k} \max \left(\left[\frac{k^{1.5}}{2.5 \varepsilon y} - 1 \right] \left[\frac{k^{1.5}}{2.5 \varepsilon y} \right]^2, 0 \right) \quad (11)$$

The various coefficients are given in table 2.

Table 2: Coefficients in k and $\tilde{\varepsilon}$ equations

$c_{\varepsilon 1}$	$c_{\varepsilon 2}$	σ_k	σ_ε
1.44	$1.92(1 - 0.3 \exp(-R_t^2))$	1.0	1.3

Numerical results and discussion

This section deals with a priori test evaluation and improvement of the EARSM model given by equation (3) in order to assess its predictive capabilities in the simulation of a fully turbulent flow through a straight square duct. To enable a correct behaviour in the regions close to the walls, damping functions of Van Driest types [9] have been used to bridge solution. These functions can be given by [10]:

$$f = (1 - a \exp(-bz^+))(1 - a \exp(-by^+)) \quad (12)$$

where z^+ ($= zu_\tau / \nu$) and y^+ ($= yu_\tau / \nu$) are the no dimensional coordinates scaled by the kinematic viscosity ν and the mean frictional velocity $u_\tau = (\tau_w / \rho)^{1/2}$, τ_w being the mean wall shear stress. The constants a and b are given in the table 3 [10]. Throughout this paper, the modified model ((3)-(11) and (12)) will be labelled Craft_f et al .

Table 3: Values of constants a and b used in the damping function f .

	$\langle u^2 \rangle$	$\langle v^2 \rangle$	$\langle w^2 \rangle$	$-\langle uv \rangle$	$-\langle uw \rangle$
a	-4.5	-5	0.91	1.01	-0.75
b	0.038	0.015	0.05	0.04	0.045

From table 3, one can note that all the normalized Reynolds stresses $\langle u_i u_j \rangle$ ($= \overline{u_i u_j} / u_\tau^2$) have different damping functions.

The a priori technique consists in using mean field turbulent coming from DNS. The mean velocity components, the turbulent kinetic energy and its dissipation rate obtained through the DNS simulations are supplied in the turbulent model, providing predictions for Reynolds stresses. The predictions are then compared with these quantities obtained directly from the DNS. The figure 3 illustrates this a priori test.

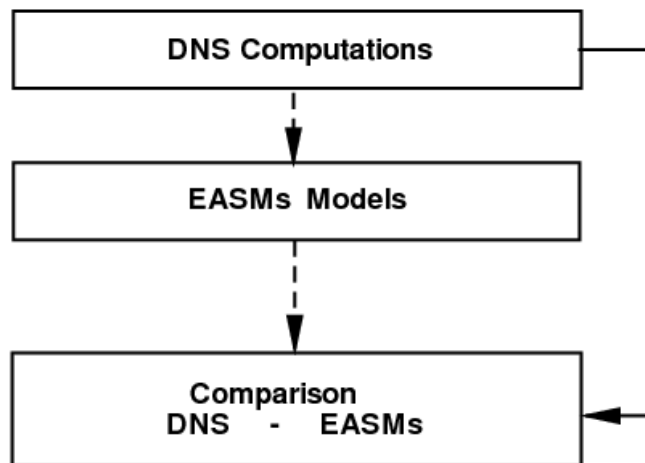


Figure 3: Schematic diagram showing the structure of a priori test.

In this paper, the comparisons are made with Gavrilakis’s DNS (1992) [3]. For this simulation, the flow variables are expanded into discrete Fourier series along the x-direction, whereas second-order centred-difference approximations are used along y and z-directions. The Adams-Bashforth scheme is used for the temporal integration. This DNS has been carried out for the Reynolds number $Re = \bar{U}_m 2h / \nu = 4800$ based on the duct height $2h$ and the mean flow velocity \bar{U}_m . The Reynolds number based on the friction velocity, $Re^+ = u_\tau 2h / \nu$, is 320. The velocity ratio \bar{U}_0 / \bar{U}_m for this configuration was 1.33, \bar{U}_0 being the mean centreline velocity. The maximum Kolmogorov scale is $1.5\nu / u_\tau$.

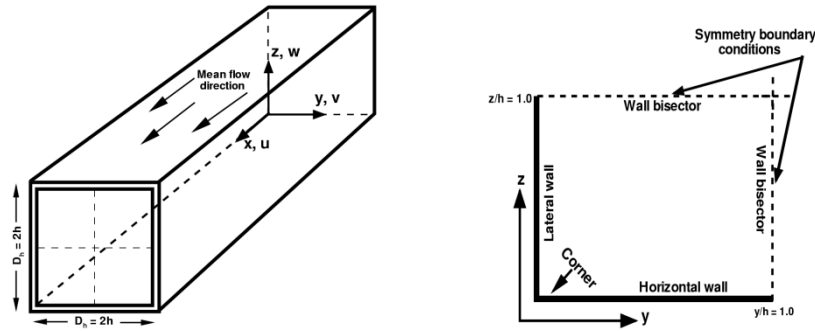


Figure 4: Flow geometry and axes system [left]; Quadrant of the square [right].

To check if the Craft et al. model reproduces the anisotropic character of the flow, a detailed analysis of the flow anisotropy may be performed via the anisotropy-invariants map proposed by Lumley and Newmann (1977) [11]. They have identified all turbulence states in terms of second (II_b) and third (III_b) invariants of the Reynolds stress anisotropy tensor b_{ij} which is defined as:

$$b_{ij} = (\overline{u_i u_j} - \frac{2}{3} k \delta_{ij}) / 2k \quad (13)$$

The second and third invariants are defined by:

$$II_b = -b_{ij} b_{ji} / 2 \quad III_b = b_{ij} b_{jk} b_{ki} / 3 \quad (14)$$

It can be shown that all the turbulence states which characterize the turbulence are limited inside the region bounded by the axisymmetric and two-dimensional states.

Figure 4 shows the variation of $-II_b$ against III_b for the Reynolds stress along the wall bisector. The tendency is towards an axisymmetric state. However, the flow behaviour is affected by the corner and the turbulence tends to a one-dimensional state. Near the duct center, the turbulence is close to isotropy.

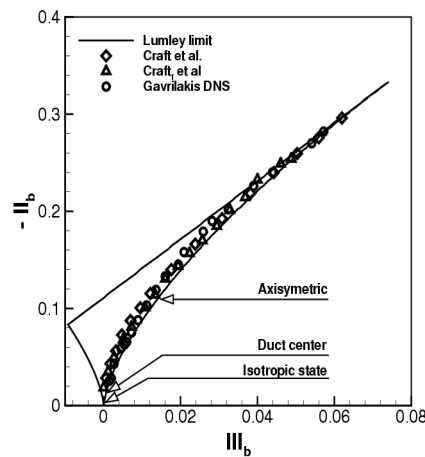
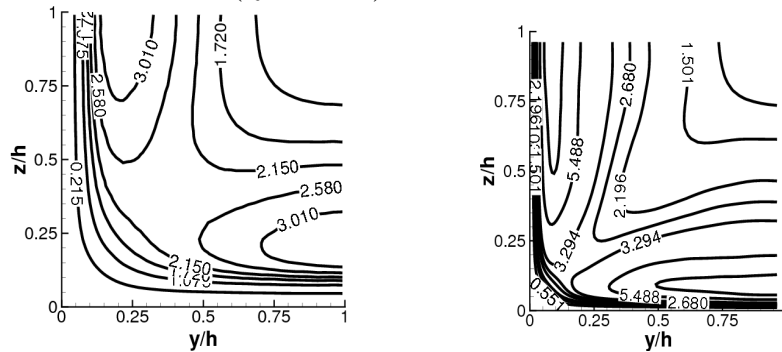


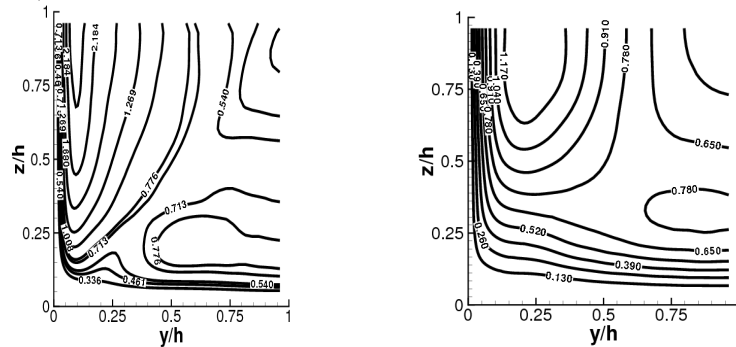
Figure 4: The trajectories in b_{ij} anisotropy map along the wall bisector.

To verify the realizability of the Craft et al. model, figures 5 and 6 present, respectively, the contours plots of the normal Reynolds stresses $\langle u^2 \rangle$ and $\langle w^2 \rangle$ and, the contours plots of the quantities $\langle uv \rangle / (\langle u^2 \rangle + \langle v^2 \rangle)$ and $\langle uw \rangle / (\langle u^2 \rangle + \langle w^2 \rangle)$. Plotted are the DNS data by Gavrilakis (1992) [3] for comparison (see figure 5(a) and 5(b)). The distributions of these quantities in the other quadrant can be obtained through a symmetric mirroring with respect to the corresponding axes or origin. By the examination of these figures, we remark that the turbulent normal stresses are positive and the Schwarz inequality is respected ($(\langle u_i u_j \rangle) / (\langle u_i^2 \rangle + \langle u_j^2 \rangle) \leq 1$). For all the Reynolds stresses, the comparison of the numerical results with available DNS shows good agreements.

In figures 7 (a, b and c), the normal profiles of the normalized turbulent stresses as a function of the z -direction along the wall bisector are represented and compared with DNS data by Gavrilakis (1992) [3] and with the model results of Speziale (1987) [12] and, Gatski and Speziale (1993) [13]. As shown in figure 7(a), the component $\langle u^2 \rangle$ is best predicted by the current EARSM model [1], although the peak is slightly underpredicted. The agreement here being satisfying, this suggest that the near wall turbulence generation mechanisms seem to be faithfully captured. One can observe that the $\langle u^2 \rangle$ component dominates the other two components with a very marked peak close to the wall ($z/h \approx 0.1$).



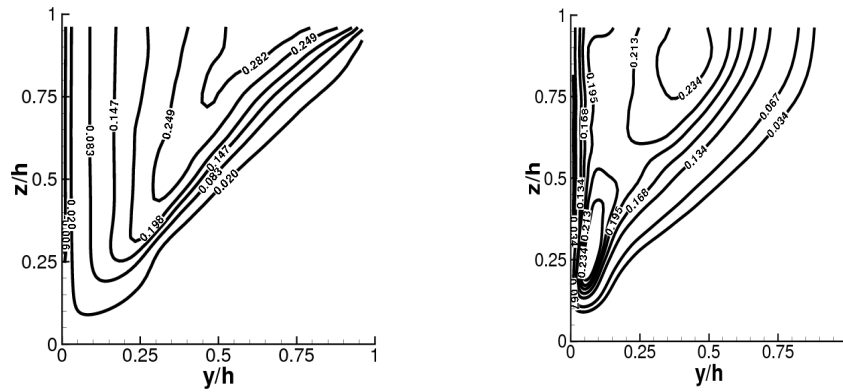
(a): the normal Reynolds stress $\langle u^2 \rangle$ [left: present study; right: data adapted from Gavrilakis (1992)]



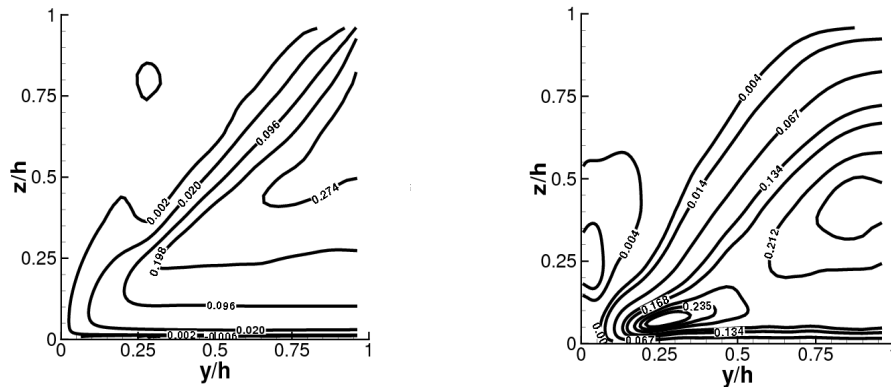
(b): the normal Reynolds stress $\langle w^2 \rangle$ [left: present study; right: data adapted from Gavrilakis (1992)]

Figure 5: Contour plots of the normal Reynolds stresses

For the y-component $\langle v^2 \rangle$ (see figure 7(b)), the Craft_f et al. model, while over-predicting the magnitude of this quantity compared with DNS from Gavrilakis (1992) [3], well duplicates the DNS far away from the wall for $z/h \geq 0.25$. Note that the peak is overpredicted by about 15% compared with the DNS and it is not reached at the same location as the DNS. Figure 7(b) clearly demonstrates that the spanwise turbulence component $\langle v^2 \rangle$ is very sensitive to choice of the model, in particular for $z/h \leq 0.25$. Also, it can be seen that its intensity increases rapidly in the near wall region, approximately corresponding to $0 \leq z/h \leq 0.1$ and that the predicted profiles are larger than the profile from the DNS. All models overpredict the magnitude of $\langle v^2 \rangle$. The vertical turbulence component $\langle w^2 \rangle$ (see figure 7(c)), in the current model agrees well with the DNS data by Gavrilakis (1992) [3] for $z/h \geq 0.30$. However, our predictions tend to slightly overestimate this intensity in the near wall region. The peak value from the present model is predicted almost at the same location as the DNS. Otherwise, some noticeable differences are found, by comparing our predictions with those of the Speziale (1987) [12] and, Gatski and Speziale (1993) [13] models. As pointed out by several authors, the main differences among the profiles of the cross-stream turbulence intensities and that of the channel flow occur in near the zones close to the walls. These discrepancies mainly affect the $\langle v^2 \rangle$ component. These may be attributed to the grid size, to the low Reynolds number used in this work and to the presence of the secondary flows in the cross-stream plane, that are absent in the case of a plane channel. Note that the Speziale model (1987) [12] is not strongly realizable. Indeed, the spanwise and the vertical turbulence intensities are negative for $z/h \leq 0.20$ (see figure 7(b) and 7(c)).



(a) : the contours plots of $\langle uv \rangle^2 / (\langle u^2 \rangle \langle v^2 \rangle)$



(b): the contours plots of $\langle uw \rangle^2 / (\langle u^2 \rangle \langle w^2 \rangle)$ [left: present study; right: data adapted from Gavrilakis (1992)]

Figure 6: Contour plots of the quantities $\langle u_i u_j \rangle^2 / (\langle u_i^2 \rangle \langle u_j^2 \rangle)$

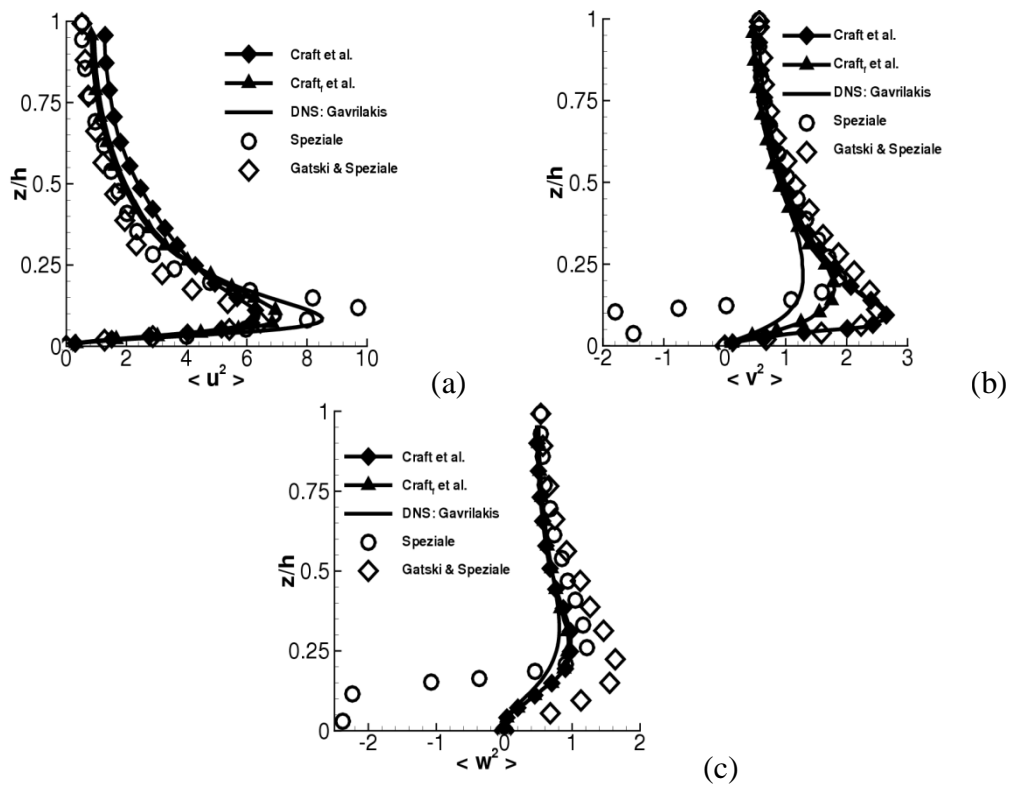


Figure 7: Normal profiles versus z/h . Comparison of Gavrilakis’s DNS (1992) with the model estimates.

Figure 8 depicts the distribution of the Reynolds shear stress component $-\langle uv \rangle$ and $-\langle uw \rangle$ along the z -direction at the wall bisector $y/h=1.0$. The current model is seen to produce much better predictions in some respects a little closer to data than

Craft et al. original form. It can be seen that the shear stress component $-\langle uw \rangle$ returned by the present model agrees well with the DNS for $z/h \geq 0.25$. This remarkable agreement obtained far from the walls is gratifying. The $-\langle uw \rangle$ peaks obtained by the two models (Craft et al. [1] and Craft_f et al) are roughly the same and they are much higher than the corresponding peak returned by DNS data.

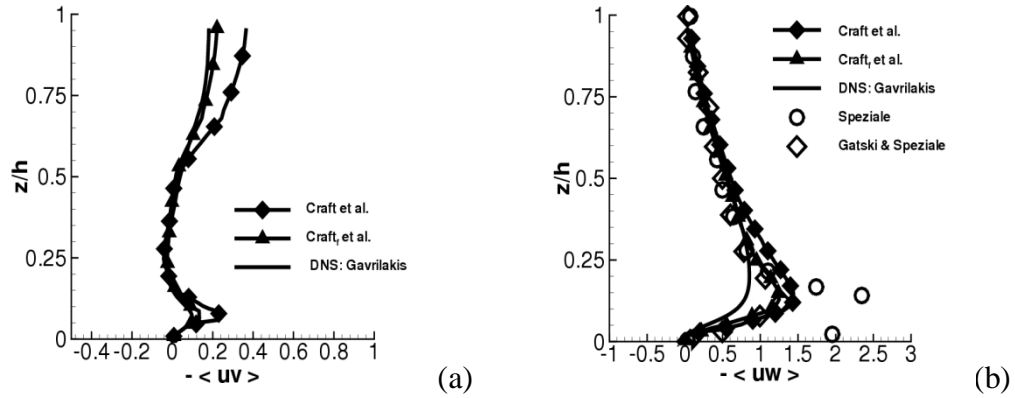


Figure 8: Shear stress profiles versus z/h . Comparison of Gavrilakis's DNS (1992) with the model estimates.

The a priori evaluation and improvement of Craft et al. model [1] shows that it is able to predict turbulence flow through a straight square duct. Therefore, the extension to a posteriori evaluation of the turbulence flow should produce reliable predictions for other similar flows at a comparable Reynolds number.

The following sub-sections are devoted to a posteriori simulation by the improved Craft_f et al. model for the case this work.

Conclusion

EARSM model is studied using a priori procedure based on data resulting from the direct numerical simulation of Gavrilakis (1992). We show that the Craft et al. model (1996) is strongly realizable, because the analysis of maps shows that the positivity of the normal Reynolds stresses and respect of the Schwartz inequalities between turbulent velocity correlations. The map of the second and third invariants for the Reynolds stress tensor indicates that within a quadrant the turbulence field comes close to one-, two-, and three-component states. To predict the significant viscous effects due to the presence of the wall and corner, damping functions are implemented. The comparison of the mean velocity field shows a good agreement. Overall, the Craft_f et al. model considered in this work yields better predictions than those obtained by the original model.

References.

- [1] Craft T. J., Launder B. E. and Suga K., 1996, "Development and application of the cubic eddy-viscosity model of turbulence", *International Journal Heat and Fluid flow*, 17, pp.108-115.
- [2] Shih T.H., Zhu J. and Lumley J. L., 1995, "A new Reynolds stress algebraic equation model", *Comp. Appl. Mech. Eng.*, 125, pp.287-302.
- [3] Gavrilakis S., "Numerical simulation of low-Reynolds-Number turbulent flow through a straight square duct", 1992, *J. Fluid Mech.*, 224, pp.101-129.
- [4] Huser A. and Biringen S., 1993, "Direct numerical simulation for turbulent flow in a square duct", *J. Fluid Mech.*, 257, pp. 65-95.
- [5] Vasquez M. S. and Métais O., 2002, "Large eddy simulation of the turbulent flow through a square duct", *J. Fluid Mech.*, 453:, pp.201-238.
- [6] Speziale C.G., Younis B.A. and Berger S.A., 2000, "Analysis and modelling of turbulence flow in an axially rotating pipe", *J. Fluid Mech.*, 407, pp.1-26.
- [7] Suga K., Abe K., 2000, "Nonlinear eddy viscosity modelling for turbulence and heat transfer near wall and shear-free boundaries", *International Journal of Heat and Fluid Flow*, 21(1), pp.37-48.
- [8] Yap C. R., "Turbulent heat and momentum transfer in recirculating and impinging flows", 1987, Ph.D thesis, University of Manchester, Manchester, UK
- [9] Van Driest E. R., 1956, "On turbulent flow near a wall, *Journal of Aeronautical Sciences*", 23, pp.1007-1011.
- [10] GNANGA H., 2008, "Analyse numérique d'écoulements turbulents anisotropes à l'aide de modèles non-linéaires de turbulence", PH. D thesis, Université des Sciences et Technologies de Lille, France.
- [11] Lumley, J. L., Newman, G., 1977, "The Return to Isotropy of Homogeneous Turbulence", *J. Fluid Mech.*, 82, pp.161-178.
- [12] Speziale C. G., 1987, On non-linear k-l and k-e models turbulence, *J. Fluid Mech.*, 178, pp. 459-475.
- [13] Gatski T. B. and Speziale C. G., 1993, On explicit stress models for complex turbulent flows, *J. Fluid Mech.*, 254, pp. 59-78.

